# Analysis of the $He^+$ on He Collision*

EDGAR EVERHART
*Physics Department, University of Connecticut, Storrs, Connecticut*
(Received 1 July 1963)

This paper is the second of two consecutive papers dealing with resonant electron capture in $He^+$ on He collisions. The first of these, by Lockwood, Helbig, and Everhart, describes differential measurements of electron capture probability $P_0$ made over a wide range of incident energy and scattering angle. The present paper treats these data within the framework of an improved theory for charge transfer due to Bates and McCarroll. The theory requires a knowledge of the energy levels of the $He_2^+$ molecular ion at all internuclear distances. Using values of these energy levels given by Lichten, the present paper computes the location of the maxima and minima of $P_0$ at all impact parameters and velocities. The repulsive potential energy of the $He_2^+$ system is also calculated here so that these impact parameters can be related to the scattering angle. These results allow the values of $P_0$ to be predicted over a wide range of impact parameters (0.05 to 1.4 Å), scattering angles ($\frac{1}{2}$ to 4°), and energies (0.4 to 1000 keV). There is fair quantitative agreement with the data curves. However, a detailed comparison of theory and data shows discrepancies. At high velocities and low impact parameters there is rather good agreement and there is again fair agreement at low velocities and large impact parameters. In between, however, at intermediate impact parameters the data curves are such that the interaction appears to be different depending on whether the velocity is above or below a critical value of about $6\times10^7$ cm/sec. This behavior of the data is not predicted by the present theory.

## 1. INTRODUCTION

THE differential scattering data of the preceding paper[1] will here be examined within the framework of the existing theory. The data show oscillations, depending on scattering angle and energy, of a quantity $P_0$, which is the probability that an incident $He^+$ ion in a single collision with a He atom will capture an electron and emerge neutral. The theory predicts a somewhat similar oscillation.

One approach to the study of these phenomena may be made through the "impact parameter method" by Bates, Massey, and Stewart,[2] by Firsov,[2] and by Holstein.[2] In the course of calculating the total cross section for charge transfer they first calculate the differential probability for charge transfer, which is another name for the probability $P_0$ under study here. The impact parameter approach has been developed further by Bates and McCarroll,[3] whose presentation is in the most useful form for the present purposes.

The oscillations in electron capture probability which are predicted by the theory are easily interpreted in terms of the following well-known qualitative picture. As the $He^+$ and He come together it is assumed that the system may be described by the normalized sum of only two wave functions of $He_2^+$. These are $\psi_g$, a function of even symmetry whose energy is $E_g$, and $\psi_u$, an odd function whose energy is $E_u$. These have different "instantaneous-time dependencies," which are $\exp(-iE_gt/\hbar)$ and $\exp(-iE_ut/\hbar)$, respectively. During the collision these wave functions get in and out of phase with an "instantaneous-beat frequency" $(E_g-E_u)/h$ which is a function of internuclear separation $R$. The beat frequency increases as the particles approach, reaches a maximum as they pass close to each other, and then drops as they recede. Since $\psi_g$ is even and $\psi_u$ odd, it is evident in adding them that when the two are in phase the extra electron is on one side, and when they are out of phase it is on the other side. Whether the extra electron finally ends up on the target or the projectile depends on the value of the "instantaneous-beat frequency" $(E_g-E_u)/h$ integrated over the collision time.

It is evident that theoretical calculations of $E_g-E_u$ for $He_2^+$ should be examined to see whether they fit the observed oscillations in electron capture probability. Such calculations of this energy difference have been made by Moiseiwitsch,[4] and extended to small values of $R$ by Lichten.[5] In fact, Lichten's work in identifying appropriate molecular wave functions and giving their energies numerically for all values of $R$ is crucial to the present comparison. At $R=0$ the system reduces to $Be^+$, and Lichten points out that a particular doubly-excited state, namely $Be^+1s(2p)^2$, should be used for $\psi_g$ at $R=0$. This state is unusual in that its energy is far above the ionization energy of $Be^+$. If Lichten's wave functions are accepted it is evident that the collisions under study here must occur in a time which is short compared to the radiative or autoionization lifetimes of this highly excited state.

In their theory, Bates and McCarroll[3] introduce and justify a velocity-dependent term which has the effect of shifting the resonant peaks of $P_0$ from the energies at

* This work was supported by the U. S. Army Research Office, Durham and the Air Force Cambridge Research Laboratories.

[1] G. J. Lockwood, H. F. Helbig, and E. Everhart, preceding paper, Phys. Rev. **132**, 2078 (1963).

[2] D. R. Bates, H. S. W. Massey, and A. L. Stewart, Proc. Roy. Soc. (London) **A216**, 437 (1953); O. B. Firsov, Zh. Eksperim. i Teor. Fiz. **21**, 1001 (1951); and T. Holstein, J. Phys. Chem. **56**, 832 (1952).

[3] D. R. Bates and R. McCarroll, Proc. Roy. Soc. (London) **245,A** 175 (1958); and Suppl. Phil. Mag. **11**, 39 (1962). In their first, paper see Eqs. (34) and (35) and in their second paper see Sec. 3.2, Eqs. (151)–(154) and Table 4, p. 74.

[4] B. L. Moiseiwitsch, Proc. Phys. Soc. (London) **A69**, 653 (1956).

[5] W. L. Lichten, Phys. Rev. **131**, 229 (1963).

which they would be found otherwise. Although this "phase" term has not been calculated theoretically for the $He^+$ on He system, such a term is clearly required by the experimental data under study here.

The present discussion of $He^+$ on He is more extensive than the earlier treatment by Ziemba and Russek,[6] which was based on much more limited experimental data and which appeared before the supporting theoretical work[5] referred to above. Resonant electron capture in a simpler collision, $H^+$ on H, has been studied experimentally by Lockwood and Everhart[7] and theoretically by Bates and McCarroll,[3] Ziemba,[8] McCarroll,[9] Ferguson,[10] and Mukherjee and Sil,[11] though there remain a number of unsolved problems for this combination. An analysis of $Ne^+$ on Ne collision data which shows a similar resonant phenomenon has been given by Jones, Costigan, and Van Dyk.[12]

The relationship between the present differential-scattering measurements of electron-capture probability and the total cross section for charge transfer are presented elsewhere in a short paper.[13]

Section 2 below briefly outlines the pertinent charge transfer theory and shows how the electron capture probability can be calculated from the appropriate wave functions of $He_2^+$ and $Be^+$. The theory gives these capture probabilities for various impact parameters and velocities, whereas the experimental capture probabilities are known for various scattering angles and velocities. Thus, to compare theory and experiment, a relationship between impact parameter and scattering angle is needed. This is calculated in Sec. 3 from an interatomic potential energy function which is consistent with the theory. A preliminary comparison of data and theory is made in Sec. 4. There a fair agreement is found at low energies as to the spacings of the resonant peaks, both in their angle and energy dependence. Section 5 presents a more detailed comparison between data and theory, and some unsolved aspects of the problem are pointed out and discussed.

## 2. THEORY

The theory for resonant charge transfer in differential scattering will be reviewed briefly and put in the most suitable form for this study. The necessary wave functions and energies of $He_2^+$ and $Be^+$ are then discussed.

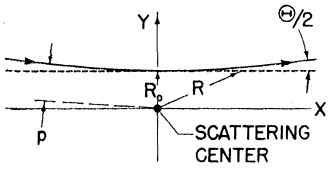


FIG. 1. A collision referred to a fixed scattering center.

This allows the electron capture probability to be calculated as a function of impact parameter and velocity.

### a. The Electron Capture Probability

There are several approximations made in developing the theory of this collision. First, it is assumed that the centers of the particles follow classical trajectories having a well-defined impact parameter. Second, as mentioned in Sec. 1 above, it is assumed that only two states of $He_2^+$ are needed in describing the system, excitation to other states being neglected. Third, the effects of rotation of the internuclear line during the collision are neglected, and fourth, an approximation is made in assuming that the wave functions at any instant are the same as they would be if the two centers were stationary at the same internuclear distance $R$. (This last assumption is, however, modified by Bates and McCarroll[3] to take account of the translational energy of the active electron and further modified by Lichten[5] to take account of the suddenness of the collision. However, in these modifications, still only two states are used to describe the system.)

Consider a particular collision at velocity $v$ wherein the two particles pass at a distance of closest approach $R_0$ as shown in Fig. 1. Subject to the approximations mentioned above, Bates and McCarroll[3] show that

$$P_0=\sin^2\zeta\,, \tag{1}$$

where

$$\zeta=\pi J(R_0)/(vh)-\pi\beta(v,R_0)\,, \tag{2}$$

and $h$ is Planck's constant. Here

$$J(R_0)=2\int_{R_0}^{\infty}(E_g-E_u)R(R^2-R_0^2)^{-1/2}dR \tag{3}$$

which is obtained by integrating the energy difference over time $t$. The $R$ dependence arises using $v^2t^2=R^2-R_0^2$. The other term, $\beta(v,R_0)$, in Eq. (2) is called the phase term and it changes slowly compared to the first term. According to the theory, $\beta$ approaches zero at low velocity.[3]

In discussing both the theory and the data it is convenient here to introduce an index $n$ related to $\zeta$ by the expression

$$\zeta=(n-\tfrac{1}{2})\pi\,, \tag{4}$$

with peaks of $P_0$, as in Eq. (1), occuring for $n=1, 2, 3, \cdots$ and the valleys for $n=\frac{3}{2}, \frac{5}{2}, \cdots$. These $n$ values are consistent with the labels given to the experimental peaks and valleys.[1] Using this expression for $\zeta$ in Eq.

---

[6] F. P. Ziemba and A. Russek, Phys. Rev. **115**, 922 (1959).
[7] G. J. Lockwood and E. Everhart, Phys. Rev. **125**, 567 (1962).
[8] F. P. Ziemba, Doctoral thesis, University of Connecticut, 1960 (unpublished), p. 36.
[9] R. McCarroll, Proc. Roy. Soc. (London) **A264**, 547 (1961). See also p. 74–75 of Ref. 3, second paper.
[10] A. F. Ferguson, Proc. Roy. Soc. (London) **A264**, 540 (1961). See also p. 74–75 of Ref. 3, second paper.
[11] S. C. Mukherjee and N. C. Sil, Indian J. Phys. **36**, 622 (1962).
[12] P. R. Jones, P. Costigan, and G. Van Dyk, Phys. Rev. **129**, 211 (1963).
[13] E. Everhart, H. F. Helbig, and G. J. Lockwood, in Proceedings of the Third International Conference on The Physics of Electronic and Atomic Collisions (to be published).

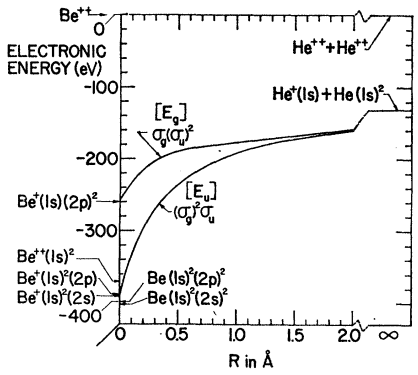


FIG. 2. Energy levels in the $He_2^+$ system versus internuclear separation. This figure is based on a similar figure by Lichten (Ref. 5).

(2), the result is

$$n(v,R_0)-\tfrac{1}{2}=J(R_0)/(vh)-\beta(v,R_0)\,, \qquad (5)$$

which is a useful expression for predicting maxima and minima of $P_0$.

The term $J(R_0)/(vh)$ in Eq. (5) largely determines the oscillations of $P_0$. At high velocities, where the impact parameter is very small, $J(R_0)$ approaches the constant value $J(0)$ for all reasonable angles of scattering $\theta$, and there the $1/v$ dependence causes the oscillations of $P_0$. However, for the low velocity collisions, even for cases where $v$ is held constant, there is a range of $R_0$ corresponding to the various scattering angles and the variation of $J(R_0)$ controls the oscillations of $P_0$.

### b. Wave Functions of $He_2^+$

In order to evaluate the integral in Eq. (3) and also in order to calculate the interatomic potential energy term in Sec. 3 below, it is necessary to know, numerically, the energies $E_g$ and $E_u$ as a function of internuclear separation $R$. These are shown in Fig. 2, which is taken from Lichten's recent paper.[5] At $R=\infty$ these energies both approach the electronic energies of the separated $He^+$ and He particles. At intermediate distances these energies are, respectively, those of the $\sigma_g(\sigma_u)^2$ and $(\sigma_g)^2\sigma_u$ states of the molecular ion. (In another notation, these are the $^2\Sigma_g$ and $^2\Sigma_u$ states.)

At $R=0$ the wave functions are those of $Be^+$ and are, respectively, those for the $1s(2p)^2$ and the $(1s)^2 2p$ state of that ion. This former state is doubly excited and lies 130 eV above the other state. It is not ordinarily seen because it lies far above the lowest state for $Be^{++}$, namely the $(1s)^2$ state. These collisions last about $10^{-16}$ sec, and this is somewhat shorter than the lifetime for autoionization ($\sim 10^{-14}$ sec) and very much shorter than radiative lifetimes ($\sim 10^{-8}$ sec). Lichten's paper is primarily concerned with the justification for using these particular states in the description of $He^+$ on He collisions, despite certain "line crossings," because of considerations having to do with the rapidity of the collisions.

The numerical values for Lichten's curves are important to the present study and so the following brief explanation is necessary here: The electronic energies for the neutral $He_2$ system are calculated for internuclear distances $R$ between 0 and 4 Å in a paper by Phillipson[14] who uses single configuration molecular orbitals. The pertinent state of Be at $R=0$ is the $(1s)^2(2p)^2$ state. Phillipson tabulates the electronic energies $\epsilon_g$ and $\epsilon_u$ which are associated, respectively, with each $1s$ and each $2p$ electron. Lichten applies Koopmans' rule,[15] which states that the corresponding energies for the ion are found by subtracting the energy associated with the missing electron. Thus, at $R=0$ the energy of the $Be^+ 1s(2p)^2$ state is that of $Be(1s)^2(2p)^2$ minus $\epsilon_g$, and the energy of the $Be^+(1s)^2 2p$ state is that of $Be(1s)^2(2p)^2$ minus $\epsilon_u$. An analogous calculation, using values tabulated in Phillipson's Tables II, III, and IV, gives the desired molecular state energies at other internuclear separations.

### c. The Energy Difference

The difference in energy $E_g-E_u$, obtained from the curves in Fig. 2 (or numerically from the values of $\epsilon_g-\epsilon_u$ in Tables III and IV of Phillipson's paper[14]), is plotted versus $R$ in Fig. 3. The values of this energy difference calculated by Moiseiwitsch[4] are also shown and there is good agreement at large $R$. The Lichten-Phillipson energy differences fit the expression

$$E_g-E_u=A\,\exp(-R/\lambda)\,, \qquad (6)$$

with $A=130$ eV and $\lambda=0.422$ Å, as indicated by the solid straight line in Fig. 3.

With this expression for the energy difference the integration Eq. (3) may be carried out analytically to yield

$$J(R_0)=2AR_0K_1(R_0/\lambda)\,, \quad \text{and} \quad J(0)=2A\lambda\,, \qquad (7)$$

where $K_1$ is the first-order modified Bessel function of the second kind. For convenience, $J(R_0)$ is tabulated in the right-hand column of Table I. At $R=0$ this has the value $J(0)=109.7$ eV-Å. It is this value which Lichten[5] compared with the experimental value of 202 eV-Å from earlier work.[16] Ziemba and Russek[6] found, partly empirically and partly by extrapolating Moiseiwitsch's values, an expression for $E_g-E_u$ which was fairly close to Eq. (6) and were the first to realize that a surprisingly high value of this energy difference, over 100 eV at $R=0$, was necessary in order to fit the data, though at the time there was no explanation of this.

[14] P. E. Phillipson, Phys. Rev. **125**, 1981 (1962).
[15] T. A. Koopmans, Physica **1**, 104 (1933).
[16] This value is tabulated in Table I of Ref. 7 where it is called $\langle Ea\rangle$, and refers to experimental work by F. P. Ziemba, G. J. Lockwood, G. H. Morgan, and E. Everhart, Phys. Rev. **118**, 1552 (1960); and Phys. Rev. Letters, **2**, 299 (1959).

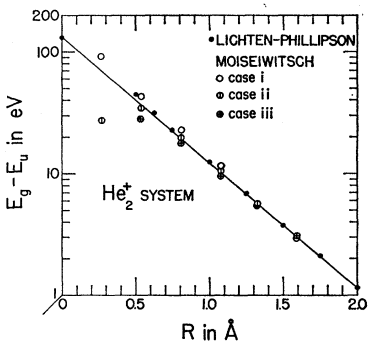


FIG. 3. The difference in energy $E_g - E_u$ between two levels in the $He_2^+$ system is plotted versus internuclear distance. The solid points are obtained following a procedure outlined by Lichten (Ref. 5) using numerical values of a related quantity in a paper by Phillipson (Ref. 14). The open circles refer to values calculated by Moiseiwitsch (Ref. 4), and the solid line is the empirical fit used in the present calculation.

## 3. IMPACT PARAMETER AND SCATTERING ANGLE

The above results depend on $R_0$ (which is very nearly the same as the impact parameter in these small angle collisions), whereas the data depend on scattering angle $\theta$. The necessary relationship between these two quantities is easily calculated numerically when the interatomic potential energy $V(R)$ is known. In the course of carrying out the calculation a functional relationship between $\theta T$ and $R_0$ appears which is, in itself, most useful in reducing the experimental data even in cases where $V(R)$ is not known.

### a. The Interatomic Potential Energy

As discussed in Sec. 1, the wave function is taken to be the sum of the two functions whose energies $E_g$ and $E_u$ are given in Fig. 2. At any particular internuclear separation $R$, the electronic energies should thus be the average of $E_g$ and $E_u$. The over-all potential energy is given by

$$V(R) = 4/R + \tfrac{1}{2}(E_u + E_g) - E(\infty), \qquad (8)$$

and equals the coulomb repulsive energy of the nuclei, plus the (negative) electronic energies, minus the (negative) electronic energies of the separated $He^+$ and He at infinity. Using the numerical values from Fig. 2, $V(R)$ may readily be calculated and the result is listed in Table I.

This table also lists an electron screening factor $g(R)$ defined as the ratio of the calculated potential to the coulomb term. Thus $g(R) = V(R)/(4/R)$, which is unity at $R=0$ and zero at $R=\infty$. There is a gap in the calculated energies $E_g$ and $E_u$ between $R=0$ and $R=0.5$ Å which was bridged in the calculation of $V(R)$ and $g(R)$ in Table I as follows: A plot of the logarithm of $g(R)$ for all $R$ fits a smooth curve whose slope becomes very slowly more negative as $R$ increases. A straight line was drawn between the points at $R=0$ and $R=0.5$ Å to determine $g(R)$ within this gap (equivalent to assuming exponential screening in this region). The slowly changing slope indicates that the often-used exponential screening function introduced by Bohr[17] is, thus, not a good over-all fit for all $R$ in this case. However, exponential screening does describe the data fairly well in some other ion-atom combinations.[18]

TABLE I. At various values of internuclear separation $R$, or distance of closest approach $R_0$, calculated values for the $He_2^+$ system are given for the potential energy $V(R)$, the screening factor $g(R)$, the product $\theta T$ of scattering angle and energy, and the integral $J(R_0)$.

| $R$ or $R_0$ (Å) | $V(R)$ (eV) | $g(R)$ (dimensionless) | $\theta T$ (deg-keV) | $J(R_0)$ (eV-Å) |
|---|---|---|---|---|
| 0 | ∞ | 1.000 | ∞ | 109.7 |
| 0.010 | 5620. | 0.976 | 330. | 109.6 |
| 0.020 | 2740. | 0.952 | 165. | 109.2 |
| 0.050 | 1020 | 0.886 | 64.7 | 107.6 |
| 0.100 | 452. | 0.785 | 31.0 | 103.3 |
| 0.200 | 177. | 0.616 | 13.8 | 92.2 |
| 0.300 | 92.8 | 0.484 | 7.96 | 80.1 |
| 0.400 | 54.6 | 0.380 | 5.09 | 68.5 |
| 0.500 | 34.3 | 0.298 | 3.45 | 57.8 |
| 0.625 | 20.2 | 0.220 | 2.24 | 46.3 |
| 0.750 | 12.0 | 0.156 | 1.49 | 36.7 |
| 0.875 | 7.13 | 0.106 | 0.973 | 28.9 |
| 1.000 | 4.06 | 0.0705 | 0.618 | 22.6 |
| 1.125 | 2.34 | 0.0457 | 0.383 | 17.6 |
| 1.250 | 1.31 | 0.0284 | 0.232 | 13.7 |
| 1.375 | 0.731 | 0.0175 | 0.135 | 10.6 |
| 1.500 | 0.401 | 0.0104 | 0.0772 | 8.21 |
| 1.625 | 0.217 | 0.00598 | 0.0429 | 6.26 |
| 1.750 | 0.108 | 0.00328 | 0.0233 | 4.80 |
| 1.875 | 0.051 | 0.00167 | 0.0123 | 3.68 |
| 2.000 | 0.024 | 0.00083 | 0.0060 | 2.81 |

Unfortunately there are no direct experimental measurements of $V(R)$ on $He^+$ on He collisions to compare with the corresponding column in Table I. The measurements of Cramer and Simons[19] were first interpreted in terms of an attractive potential which would give the observed scattering, but Mason and Vanderslice[20] showed that these same measurements could equally well be used to determine a repulsive potential. Their results, however, are not in a form which can be compared with $V(R)$ in Table I.

### b. Small Angle Scattering

Using $V(R)$, the scattering angle corresponding to a given impact parameter and energy is readily calculated. It is well known that a classical calculation is valid[2,21] insofar as the trajectories of the particles are concerned.

Consider the scattering of a particle of reduced mass

[17] N. Bohr, Kgl. Danske Videnskab. Selskab. Mat. Fys. Medd. **18**, 8 (1948). See part 1.4, Eq. (1.4–1).

[18] E. N. Fuls, P. R. Jones, F. P. Ziemba, and E. Everhart, Phys. Rev. **107**, 704 (1957); G. H. Lane and E. Everhart, *ibid.* **120**, 2064 (1960).

[19] W. H. Cramer and J. H. Simons, J. Chem. Phys. **26**, 1272 (1957).

[20] E. A. Mason and J. T. Vanderslice, Phys. Rev. **108**, 293 (1957).

[21] E. Everhart, G. Stone, R. J. Carbone, Phys. Rev. **99**, 1287 (1955).

$\mu$, velocity $v$, from potential $V(R)$, through a small angle $\Theta$ from a fixed scattering center as in Fig. 1. For the purpose of computing the sideways force during the collision the force along the actual path, shown solid, is taken as equal to the force along the dotted straight line which lies at the same distance $R_0$ from the scattering center. The ratio of the sideways impulse during half the collision to the initial momentum must be half the scattering angle. Thus,

$$\tfrac{1}{2}\Theta=\mu v_y/(\mu v)=\int_0^\infty\left(\frac{-dV}{dR}\right)\left(\frac{R_0}{R}\right)\frac{dt}{(\mu v)}, \tag{9}$$

or

$$\Theta(\tfrac{1}{2}\mu v^2)=\int_{R_0}^\infty\left(\frac{-dV}{dR}\right)R_0(R^2-R_0^2)^{-1/2}dR, \tag{10}$$

where the relationship $R^2=R_0^2+v^2t^2$ is again used to change an integral over time $t$ to the corresponding integral over $R$.

From Eq. (10) it is evident that the product of angle and energy in the inertial frame is a function only of $R_0$. The conversion to the laboratory frame, wherein the kinetic energy is $T$ and the scattering angle is $\theta$, involves proportionality constants which only depend at small angles on the mass ratio of the colliding particles. Thus, for small angle collisions,

$$R_0=R_0(\theta T). \tag{11}$$

This is a most useful general result since it is independent of the form of $V(R)$. A given line of constant $\theta T$, as indicated by the lines so marked in Figs. 4 and 6 of the preceding paper,[1] includes all data for a fixed $R_0$. Different points along this line correspond to differing values of the velocity. The result will be used in Sec. 5 below. Equation (11) was derived also by Jones *et al.*,[12] and they used the above principles in their analysis of $Ne^+$ on Ne collisions.

### c. Dependence of $R_0$ on $\theta$ and $T$

The next step is to carry out a numerical integration of Eq. (10) for the particular $V(R)$ function in Table I. [The subsequent conversion to the laboratory frame is easy, since $\theta=\frac{1}{2}\Theta$ and $T=2(\frac{1}{2}\mu v^2)$ in this case.] The result is given in Table I which shows $\theta T$ in deg-keV as a function of $R_0$ in angstroms. This relationship is an important link in relating the data to the theory in the next section.

## 4. PRELIMINARY COMPARISON OF THEORY AND DATA

The family of curves shown by the data in Fig. 4 of the preceding paper[1] will be calculated entirely theoretically. The problem is to calculate the contours of constant $n$, which are the maxima and minima of $P_0$, on coordinates of kinetic energy $T$ versus scattering angle $\theta$. For the present the phase-term $\beta$ will be taken as zero, since this term has not been evaluated theoretically. The results should be valid at low energies where the theory predicts that $\beta$ approaches zero.

### a. Calculation Procedure

Setting $\beta=0$ in Eq. (5) and using quantities tabulated in Table I, the desired relationship between energy, scattering angle, and peak number $n$ is readily obtained. As an example of the procedure, consider a collision where $R_0=0.5$ Å. Corresponding to this value, Table I yields $\theta T=3.45$ deg-keV and $J=57.8$ eV-Å, or $92.5\times10^{-20}$ erg-cm. Choosing (say) $n=6$, it is found, upon substituting into Eq. (5) that $v=0.253\times10^8$ cm/sec, whence $T=1.34$ keV. Since $\theta T$ is known, $\theta$ is 2.57°. This determines the coordinates $T$, $\theta$ of one point on the $n=6$ contour. Choosing other values of $n$ at this $R_0$, and then repeating the process for other values of $R_0$, the entire $T$ versus $\theta$ plane can be covered with contours of constant $n$.

The result of this calculation is shown by the dotted lines in Fig. 4 here. Also shown on this figure are solid lines from the data of Fig. 4 of the preceding paper.[1]

### b. Discussion

The calculated curves of Fig. 4 are of the same over-all form as the data curves and have roughly the same spacings. The theory, even with $\beta$ set equal to zero, is a useful first approximation.

At high energies, where the curves are independent of $\theta$, the calculated and measured lines are widely displaced from each other. This is a consequence of setting $\beta=0$. If $\beta$ had been chosen equal to 0.32, then the calculated curves would fit the data fairly well at high energies, but the agreement at low energies would not be improved.

At low energies, where $\beta$ should be small, the calcu-

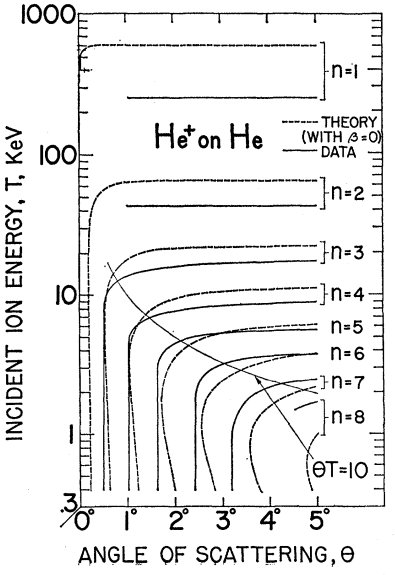


FIG. 4. The locations of the maxima of electron capture probability $P_0$, labeled by their identifying indices $n$, are plotted on coordinates of incident energy $T$ versus angle of scattering $\theta$. The solid lines are from the data (Ref. 1) and the dotted lines are calculated in the present paper.

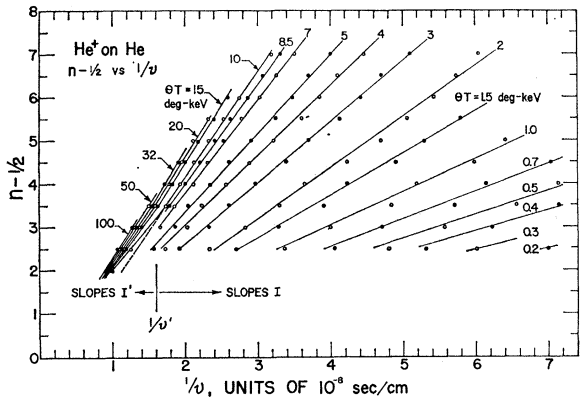


FIG. 5. A quantity $n-\frac{1}{2}$, (where $n$ is an index identifying the several maxima and minima of electron capture probability) is plotted versus reciprocal velocity $1/v$. For each line the product $\theta T$ of angle and energy has the constant value given. For $\theta T<10$ straight lines are drawn through the data points. However, for $10\leq\theta T\leq 32$ the line is bent at about $1/v'$ as shown and the data is there approximated for each $\theta T$ by two straight lines of different slopes, one above and one below the value $1/v'$.

lated curves are displaced and distorted away from the data curves. In particular, the remarkably straight data curves parallel to the $T$ axis in the lower left part of Fig. 4 are not predicted.

## 5. DISCUSSION OF $J$ AND $\beta$

Working with the data, it is possible to obtain values for terms which should be related to both $J$ and $\beta$ and these values may suggest the direction for improvements in the theory.

### a. Reduction of the Data

The key to the interpretation of the data is that it is possible to consider, separately, the subsets of data which correspond to fixed values of the impact parameter. The general functional relationship of Eq. (11) indicates that this subset is that wherein $\theta T$ is held constant. Consider, for example, the particular hyperbola $\theta T=10$ deg-keV shown on Fig. 4 here, (but shown best with the data points on Fig. 4 of Ref. 1). Along this line of constant impact parameter, the experimental values of $n$ and $v$ are known. It is useful to plot $n-\frac{1}{2}$ versus $1/v$ for these data, as shown by the line marked $\theta T=10$ on Fig. 5. The ordinate, $n-\frac{1}{2}$, measures the number of periods of oscillation of charge during the collision in question, and the abscissa $1/v$ is proportional to the duration of the collision. Lines are plotted on Fig. 5 for many other fixed-impact parameters. The smallest impact parameter or $R_0$ value is represented by the $\theta T=100$ line and the largest $R_0$ value by the data point for $\theta T=0.2$.

Within the scatter of the data points many of the lines through the data on Fig. 5 are straight and may be represented by an equation

$$n-\tfrac{1}{2}=I/(hv)-B, \qquad (12)$$

where the slope $I$ and the intercept $B$ depend on $\theta T$, but are not functions of velocity $v$. Planck's constant is inserted here so that Eq. (12) will have the same general form and dimensions as Eq. (5).

The experimental values of $I$ and $B$, determined from straight lines drawn through the data points on Fig. 5, are plotted as functions of $\theta T$ in Fig. 6(a), (b). For most of the data where $\theta T<10$ there is no difficulty, but the data for $\theta T=2$ curves upward in Fig. 5 and does not fit a straight line very well. Since this upward curve is not confirmed by data for adjacent values of $\theta T$, this may be due to data scatter. At very low $\theta T$, whenever there are enough points to determine a line, this line in Fig. 5 appears to go through the origin. For $\theta T=0.3$ and 0.2, where there are only two data points, the line is drawn through the origin to determine the slope $I$.

The data for $\theta T=10$, 15, 20, and 32 do not fit single straight lines, but are consistent with each other. In each case the slope, which is fairly constant up to a particular value of reciprocal velocity, namely $1/v'$ which is about $1.6\times10^{-8}$ sec/cm, definitely increases at higher values of $1/v$. The velocity and energy corresponding to $1/v'$ are $v'=6\times10^7$ cm/sec and $T'=8$ keV, respectively. In these cases a fairly well-defined slope $I'$ and intercept $B'$ are obtained below $1/v'$. An average slope $I$ and intercept $B$ are then obtained for the best straight line through the data points above $1/v'$.

It must be pointed out that the present interpretation

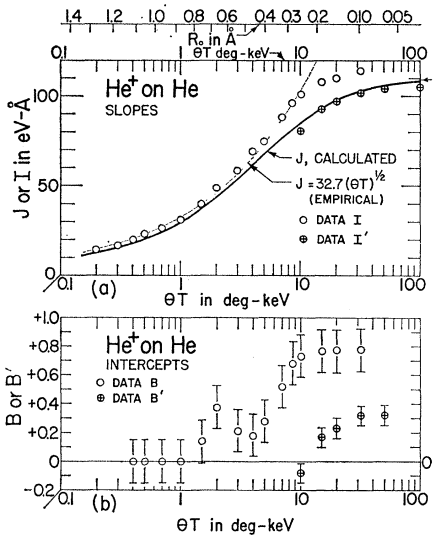


FIG. 6. (a) The slopes $I$ and $I'$ of the lines in Fig. 5 are plotted versus the parameter $\theta T$. The double values arise because the lines in Fig. 5. are bent at a particular value $v'$ of velocity. Here $I$ refers to slopes for velocities below $v'$ and $I'$ applies to velocities above $v'$. The heavy solid curve for a comparable theoretical quantity $J$ is calculated from the present paper. The arrow on the right margin indicates the value of $J$ for infinite $\theta T$. The dashed curve is an empirical fit to the low $\theta T$ data and follows the equation $J=32.7(\theta T)^{1/2}$. Along the upper edge are indicated the values of $R_0$, the distance of closest approach, which correspond to the values of $\theta T$. (b) The values of the intercepts $B$ and $B'$, obtained from the lines in Fig. 5 are plotted versus $\theta T$.

is not the only way the data could be handled. For example, the line for $\theta T=20$ in Fig. 5 could equally well be broken into three segments of different slopes and the scatter of the data points is such that this alternative could be defended if that particular $\theta T$ line were alone considered. However, the adjacent lines for $\theta T=7$, 8.5, and 10 are essentially straight above $1/v'$, consistent with the present interpretation of the cases $\theta T=15$, 20, and 32. In any case, nothing is known about the lines in Fig. 5 beyond the range there indicated and it should not be inferred that the slopes and intercepts $I$, $I'$, $B$, and $B'$ of Fig. 6 apply beyond the limits of the present data.

### b. Comparison of Data and Theory

It is by no means clear that there is necessarily a one-to-one correspondence between the experimental $I$ of Eq. (12) and the theoretical $J$ of Eq. (5). Thus, $\beta$ in Eq. (5) is not purported to be independent of $v$, and if it included a term proportional to $1/v$, this term should be included with $J$ in predicting the slopes $I$ measured experimentally. For the same reason $\beta$ is not directly comparable with $B$. Nonetheless, it should be interesting to compare the calculated $J$ values with the experimental slopes $I$. Thus the solid line in Fig. 6(a) is drawn to show the values of $J$ from Table I plotted versus $\theta T$. For convenience, the calculated $R_0$ values from Table I are also indicated along the upper edge of Fig. 6(a).

On the right side of Fig. 6(a), for $\theta T>10$, the slopes $I'$, which refer to data taken above 8 keV, fit the calculated $J$ curve fairly well, but the slopes $I$, which refer to the lower energy data, do not agree. The agreement between $J$ and $I'$ in this region may be significant despite the fact that the phase terms $\beta$ and $B$ are here neither zero nor necessarily equal. The value of $J$ at high $\theta T$ values approaches $J(0)$, which equals twice the area between the curves $E_g$ and $E_u$ of Fig. 2. This agreement between the high-energy data (>8 keV) and the calculated values of $J$ indicates that this area may be substantially correct. However, this conclusion is not completely certain because neither the double set of slopes, $I$ and $I'$, nor the interrelationship of $\beta$ and $B$ is understood. These topics are discussed further in Sec. 4c below.

The situation is, happily, more clear-cut at small values of $\theta T$ in Fig. 6(a), where the measured slopes $I$ fit the calculated slopes $J$ fairly well for $\theta T<1$. In this region of large impact parameter (where the data generally correspond to low velocity collisions also) it is predicted that $\beta$ should be zero, and it is seen in Fig. 6(b) that $B$ is zero also. Under these conditions $J$ and $I$ should indeed be comparable. The values of $J$ in this region depend mostly on the detailed shape and values of the $E_g-E_u$ curve of Fig. 3 at values of $R$ greater than about 0.85 Å, and to a lesser extent on the $V(R)$ curve for this same region in $R$. The observed slopes $I$ are only about 10% higher than the calculated $J$ curves and this indicates that the theory is substantially correct in this region.

The dashed curve fitted to the data points has the equation

$$J=32.7(\theta T)^{1/2} \tag{13}$$

with $J$ in eV-Å and $\theta T$ in deg-keV. This equation, as discussed in Sec. 4 of the preceding paper,[1] is consistent with an empirical relationship that fits the experimental data very well at low values of $\theta T$.

### c. Discussion

The velocity dependence which results in the two average slopes $I$ and $I'$ in Fig. 6(a) may indicate a breakdown in the adiabatic or diabatic description of this collision. It is strange that the present theory fits fairly well at both the high-velocity limit and at the low-velocity limit, but is difficult to reconcile with the data in between.

Adjusting the value of the $\beta$ term can bring theory into agreement with experiment. Thus, if the calculated $J$ values are used in Eq. (5), along with the experimental values of $n$ and $v$, it is easy to determine a value of $\beta(v,R_0)$ which will reconcile these. Such a calculation was carried out and it was easily seen that a linear relationship of $\beta$ with $1/v$, with a relatively sudden change of slope at the critical value $1/v'$ would reproduce any of the broken lines for $10\leqslant\theta T\leqslant 32$ on Fig. 5. However, the scatter of the data points in Fig. 5 is large enough so that no other regularities were noted in this trial adjustment of $\beta$. The family of curves $\beta$ versus $1/v$ for various $\theta T$ were sufficiently erratic that it is not worthwhile to reproduce them here.

### d. Unsolved Problems

Further theoretical work is needed in predicting the values of $\beta$. There have been no such computations for $He^+$ on He but this calculation has been carried out for the $H^+$ on H system by Ferguson[10] and by McCarroll[9] as a step in the calculation of the total cross section for charge transfer in that system. However, these intermediate results for $\beta$ are not presented in their papers.

Another unsolved problem is to account for the fact that the peaks and valleys of $P_0$ do not go from zero to unity as predicted by Eq. (2), but have a smaller range as seen by Figs. 2 and 3 of the preceding paper.[1] Perhaps this is caused by excitation to other states. The two-state approximation may be an over-simplification. This must, in fact, be the case because, at energies in excess of 10 keV, $He^{++}$ constitute several percent of the scattered particles.[1] Thus, the resonant electron-capture effect is seen in the presence of ionization and excitation in a fraction of the collisions.

The theoretical $J(\theta T)$ curve compared here with the data in Fig. 6(a) is the result of two calculations which are relatively independent of each other. The first of these calculations is to find $J(R_0)$ using Eq. (3), and

this depends on the adopted energy difference $E_g(R) - E_u(R)$. The second calculation is the conversion from $R_0$ to $\theta T$. This second step need not be carried out theoretically since it is amenable to an experimental solution. Single collision measurements of the scattering outside a given fixed angle of scattering would lead rather directly to the desired relationship between impact parameter and scattering angle. In such a measurement of $He^+$ on He scattering, all scattered incident particles including both the $He^+$ and the He component should be counted. Both elastic scattering and charge transfer here are "elastic" processes in the sense that there is no energy loss and the scattering potential energy $V(R)$ is the same for both scattered components.

### e. Comparison with $H^+$ on H and Other Cases

Despite the several discrepancies between theory and data which are seen here, the over-all agreement in the present three-electron case is surprisingly good in view of the complexity of the problem. There is little to be gained at present in further improving the values of the energy levels of $He_2^+$ without first making a significant advance in the basic theory.

In the one-electron case, $H^+$ on H, which is simpler theoretically[3,8–11] but more difficult experimentally,[7] there remain differences between theory and data which are at least as large as those observed in the present paper. Inasmuch as the $H_2^+$ wave function energies are known exactly, these differences again indicate that the basic charge-exchange theory must be improved. However, even if the $H^+$ on H case were some day completely and exactly understood, it would still be necessary to study the $He^+$ on He case and other multi-electron cases in detail. As seen here the energy level diagrams involve line crossings and multiply excited states which have no counterpart in the one-electron case. A partial understanding of the $He^+$ on He case should be useful in understanding the $Ne^+$ on Ne and $Ar^+$ on Ar cases which are known[12] to exhibit very similar resonant electron-capture phenomena.

### ACKNOWLEDGMENTS

The author is indebted to Professor Arnold Russek for his continuing interest and advice and to Dr. Grant Lockwood and Herbert Helbig for contributions towards better understanding of the experimental data.

Professor D. R. Bates of Queens University (Belfast), Professor W. L. Lichten of the University of Chicago, Professor T. A. Green of Wesleyan University, Professor P. E. Phillipson of the University of Michigan, and Professor P. R. Jones of the University of Massachusetts, have been most kind and helpful in their discussion of various aspects of the theory.